

Transitional Gas Jet Diffusion Flames in Microgravity

Ajay K. Agrawal¹, Khalid Alammari², and S.R. Gollahalli¹

¹School of Aerospace and Mechanical Engineering

University of Oklahoma, Norman, OK 73019

²Department of Mechanical Engineering

King Saud University, Riyadh, Saudi Arabia, 11421

Drop tower experiments were performed to identify buoyancy effects in transitional hydrogen gas jet diffusion flames. Quantitative rainbow schlieren deflectometry was utilized to optically visualize the flame and to measure oxygen concentration in the laminar portion of the flame. Test conditions consisted of atmospheric pressure flames burning in quiescent air. Fuel from a 0.3mm inside diameter tube injector was issued at jet exit Reynolds numbers (Re) of 1300 to 1700. Helium mole percentage in the fuel was varied from 0 to 40%. Significant effects of buoyancy were observed in near field of the flame even-though the fuel jets were momentum-dominated. Results show an increase of breakpoint length in microgravity. Data suggest that transitional flames in earth-gravity at $Re < 1300$ might become laminar in microgravity.

Introduction

Transition from laminar to turbulent combustion has been the subject of several investigations. The classical study of Hottel and Hawthorne¹ identified a sudden breakdown of laminar flame above a certain fuel injection velocity. Then, the flame comprised of an upstream laminar region and a downstream turbulent region, separated at the breakpoint. The distance from the injector exit to the breakpoint, termed breakpoint length, decreased asymptotically with an increase in the fuel injection velocity. Experiments by Takeno and Kotani² show two turbulence-generating mechanisms in the flame, also described by Gaydon and Wolfrum³; flow fluctuations inside the fuel injector and hydrodynamic instability in the shear layer of the fuel jet. They found that transition in hydrogen flames occurred by instability of the jet shear layer at fuel jet exit Reynolds number (Re) much below the critical Reynolds number ($= 2000$) for turbulent pipe-flow. In this case, the laminar fuel jet undergoes transition to turbulence, similar to that in cold jets. As the turbulent fuel-jet spreads out in an inverted cone shape, it interacts with the flame zone causing the flame to become turbulent. A sudden increase in flow mixing by turbulence shifts the flame surface inwards at the breakpoint. Takeno and Kotani² found that transition in acetylene flames did not occur at Re below the critical Reynolds number. Flames transitioned at $Re > 2000$ by the pipe-flow turbulence interacting with the flame zone. Similar observations were made by Takahashi et al.⁴, who studied transition in pure and nitrogen-diluted hydrogen flames from tube burners.

The presence of turbulence in the injector does not always result in flame transition because mixing of the

fuel jet with the surrounding high-viscosity combustion products may dissipate the turbulence. Coats and Zhao⁵ found that a contoured nozzle injector was more effective in dissipating fuel flow fluctuations as compared to a parallel-sided tube injector, presumably because of the smaller flow fluctuations at the nozzle exit. They also found that the buoyancy-induced coherent vortices outside the flame sheet^{6, 7} were not responsible for transition from laminar to turbulent combustion. The latter observation is supported in studies reviewed by Takeno⁸.

Hegde et al.⁹ employed microgravity environment to isolate buoyancy effects on flow transition in jet diffusion flames using propane, propylene, and methane fuels. Both the buoyant and nonbuoyant flames transitioned at Re above the critical Reynolds number, suggesting that the turbulence originated from inside the injector. They observed that transition in microgravity affected the entire flame, as opposed to the earth gravity transition that disturbed the flame region only downstream of the breakpoint. Based on the computed flow fields in earth and microgravity, Hegde et al.⁹ argued that a disturbance would be amplified most near the flame base in microgravity and towards the flame tip in earth gravity, as observed.

The literature review shows only one study of buoyancy effects on flame transition⁹ arising from turbulence inside the fuel injector. In the present study, we consider buoyancy effects on flame transition arising from hydrodynamic instability in the shear layer of the fuel jet. In particular, we investigate transitional hydrogen gas jet diffusion flames in earth and microgravity at jet exit Reynolds numbers varying from 1300 to 1700. The fuel jets are momentum-dominated with jet exit Froude numbers in earth-

¹ Corresponding Author: aagrawal@ou.edu

gravity varying from 7.4×10^7 to 1.3×10^8 . Flames were visualized using quantitative Rainbow Schlieren Deflectometry or RSD, a line-of-sight measurement technique developed by Greenberg et al.¹⁰ The following sections describe the experimental approach, results and discussions, and conclusions.

Experimental Approach

Experiments were performed in the 2.2-second drop-tower facility at the NASA Glenn Research Center. A drop rig housed the experiment including fuel supply and ignition systems, the RSD apparatus, and data acquisition and control systems. The fuel supply system consisted of an onboard 1000-ml vessel, a pressure regulator, a relief valve, shut-off valves, a mass flow meter, a solenoid valve, and a tube burner. A small plenum was provided upstream of the burner to damp out the flow fluctuations. The burner was a straight stainless-steel tube of 0.305mm ID with length-to-diameter ratio of at least 50 to ensure fully developed flow at the discharge. The fuel jet issued vertically into open atmosphere of the drop rig. The fuel was ignited by a retractable spark-igniter.

The RSD apparatus was mounted on a stainless steel breadboard. A 5- μ m wide, 3-mm high source aperture was placed at the focal plane of a 80-mm diameter, 310-mm focal length achromatic lens. A 600- μ m diameter fiber optic cable connected to a 150-W halogen light source provided the light input to the source aperture. Light rays were decollimated by a 80-mm diameter, 1000-mm focal length achromatic lens. A pair of mirrors was used to fold the light rays by 180 degrees. A displaced image of the source was formed at the focal plane of the decollimating lens, where a 2.5-mm wide symmetric color filter was placed. A 75-mm focal length camera lens was used to image the test section onto the CCD array of the video camera. Real time schlieren images from the camera were digitized by 24-bit color frame grabber installed in an onboard Pentium 166 MHz computer operating under Windows 95. The system RAM stores about 6 seconds of images in TIFF format, at pixel resolution of 640x480.

The experiment was integrated and controlled by the computer. The computer fans were turned-off prior to the drop to minimize flow fluctuations. Next, the fuel was turned on, and the flame was ignited and allowed to reach steady state. Then, the drop was initiated while acquiring and digitizing schlieren images. After impact, the computer fans were turned on and the fuel supply was cut off. After rig recovery, the image data from computer memory were transferred to an external data-storage device for post-processing. In post-processing, the hue (color) measured from the schlieren image was converted to angular deflection using filter calibration. The refractive index was found by Abel inversion of

angular deflection data. The oxygen concentration is determined from refractive index using state-relationships assuming chemical equilibrium in the flame. Details of the analysis procedure and measurement uncertainties are given by Al-Ammar¹¹.

Results and Discussion

In this section, we depict the flame structure using angular deflection i.e., the refractive index (or density) gradient integrated along the line-of-sight, deduced from color schlieren images. Figure 1 shows contours of angular deflection in earth and microgravity flames at $Re=1700$. The jet exit Froude number in earth-gravity (Fr) was 1.3×10^8 . The microgravity data corresponded to the last schlieren image prior to the impact in the drop tower. The spatial coordinates are normalized by the burner inside diameter. Both the earth and microgravity flames in Fig. 1 show a breakpoint marked by an inward shifting of the flame flow-field. Regardless of the gravity, the transition from laminar to turbulent combustion was triggered by the fuel jet instability. Figure 1 reveals a small, yet noticeable, increase of breakpoint length in microgravity. Significant buoyancy effects are apparent in the hot-product region surrounding the momentum-dominated fuel jet in the near field. The schlieren boundary, demarcating the heated flow of the flame from the surrounding air, is wider in microgravity (28d) as compared to that in earth-gravity (23d). In addition, the axial diffusion upstream of the injector exit is more prominent in the absence of gravity. Buoyancy effects are not obvious in the turbulent region, showing the combustion products spreading at an angle (based on the schlieren boundary) independent of the gravity. The latter suggestion was based on data taken for z/d up to 180 but not shown in Fig. 1.

The next two figures depict the effects of Re on flame transition in earth and microgravity. Figure 2 shows angular deflection contours for $Re=1500$ and $Fr=1.0 \times 10^8$. Evidently, the increase in the breakpoint length with a decrease in Re , known to exist in earth gravity flames, persists in microgravity flames. A lack of buoyant acceleration has increased the laminar flame width in microgravity. The transition from laminar to turbulent combustion occurs farther downstream in the absence of gravity. Buoyancy effects were prominent at $Re=1300$ and $Fr=7.6 \times 10^7$ as shown by the angular deflection contours in Fig. 3. In this case, the laminar flow region in microgravity was almost twice as wide as that in earth-gravity. Note that the scale in Fig. 3 is different from that in Figs. 1 and 2, to depict the wider flames.

Figure 4 shows the oxygen concentration profiles in the laminar portion of transitional flames in earth and microgravity. The profile at different Reynolds

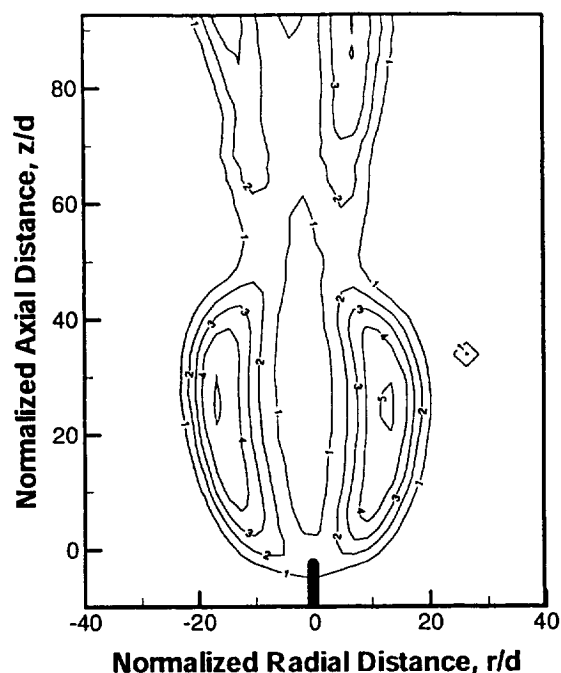


Fig. 1a Angular Deflection Contours in Earth-g, $Re=1700$

numbers are shown at an axial distance normalized by Re . At $Re=1300$, the flame radius marked by zero oxygen mole fraction region increased from $r/d=4$ in earth gravity to $r/d=8$ in microgravity. Figure 4 depicts smaller radial gradients of oxygen concentration in microgravity. Unlike the laminar flames, it is shown that the profiles in earth and microgravity depend on the Re at an axial location normalized by the Reynolds number.

Figure 5 show the breakpoint length as a function of the Reynolds number. Here, it is shown that the breakpoint length decreases asymptotically with increasing Reynolds number in both earth and microgravity. In addition, the difference between earth and microgravity breakpoint lengths increases with decreasing Reynolds number. It is therefore possible that at some Reynolds number below 1300, a transitional flame in earth-gravity will become laminar in microgravity. We could not explore this possibility in the present study because of the limited field-of-view of the schlieren apparatus.

The above results suggest that buoyancy in the flame destabilizes the fuel jet. This effect may be attributed to an increase in the effective Reynolds number because of the increase in velocity by buoyant acceleration in earth gravity⁹. Note that the effective Reynolds number proposed by Takeno and Kotani² employs fuel jet properties in the flame region to account for the effects of heat release. The increased

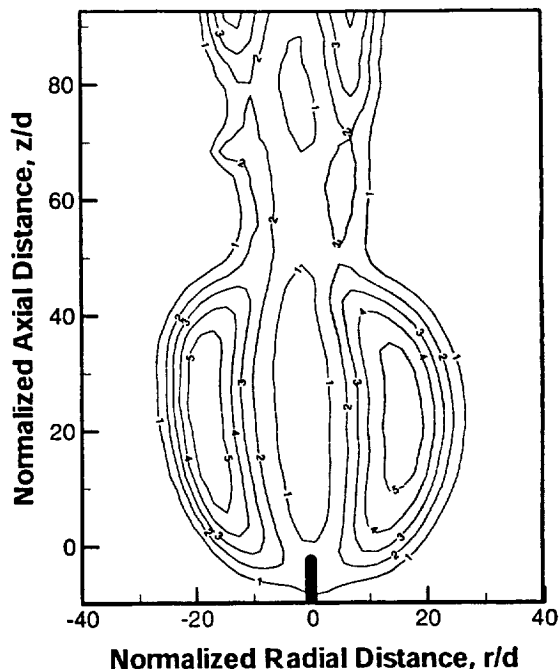


Fig. 1a Angular Deflection Contours in Micro-g, $Re=1700$

separation distance between the fuel jet and flame zone may also account for the longer breakpoint distance in microgravity. This is because the turbulent fuel jet must spread farther to interact with the flame surface.

To further examine buoyancy effects on flame transition, the heat-release in the flame was varied by diluting hydrogen with helium. Unlike nitrogen or other heavy inert gases used in past studies of hydrogen flames in earth gravity, helium was used in this work to minimize the differential diffusion and associated changes in the flame structure. Figure 6 shows contours of angular deflection in earth and microgravity for $Re=1700$ and helium mole fraction in fuel of 0.4. Here, the radial flow domain is smaller than that using pure fuel (see Fig. 1). This is because of the smaller stoichiometric air fuel ratio of the diluted fuel. The transition region has also shifted downstream with the addition of diluent in the fuel. This shift is perhaps caused by a lower effective Reynolds number resulting from the dilution. Figure 6 depicts only minor effects of gravity on the radial flow domain. The buoyancy, however, has a noticeable effect on the breakpoint length, which increases in microgravity.

Figure 7 shows the breakpoint length as a function of helium mole fraction in the fuel for $Re=1700$. Here we notice that the breakpoint length increases with increasing dilution, and that the difference between earth and microgravity breakpoint lengths increases with increasing helium mole fraction in the fuel.

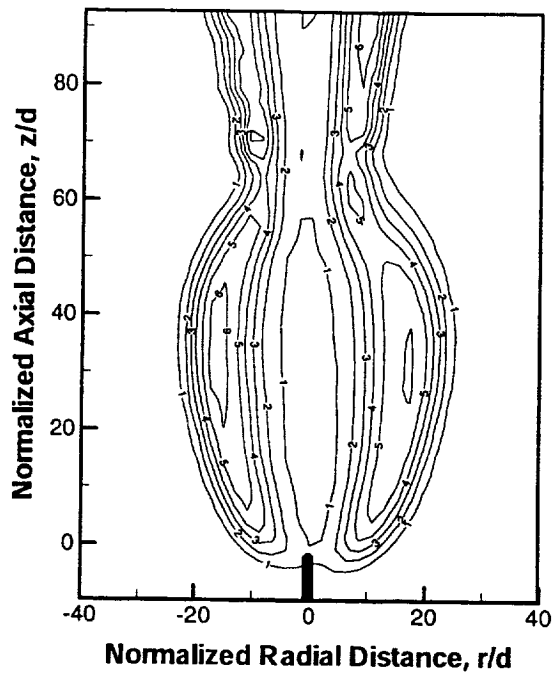


Fig. 2a Angular Deflection Contours in Earth-g, $Re=1500$

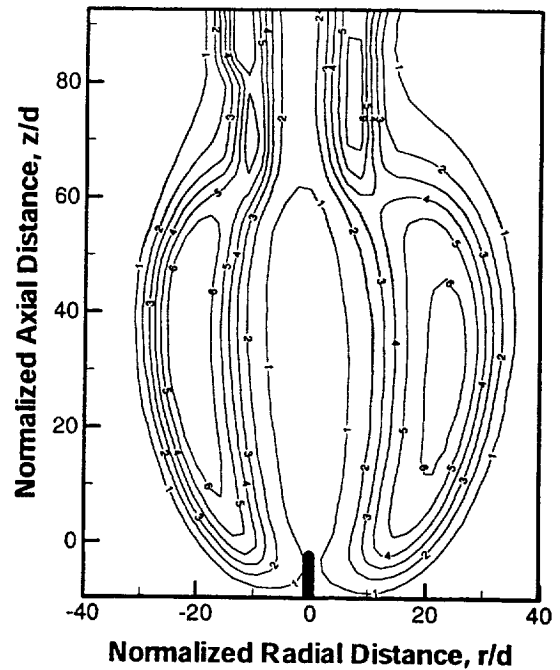


Fig. 2b Angular Deflection Contours in Micro-g, $Re=1500$

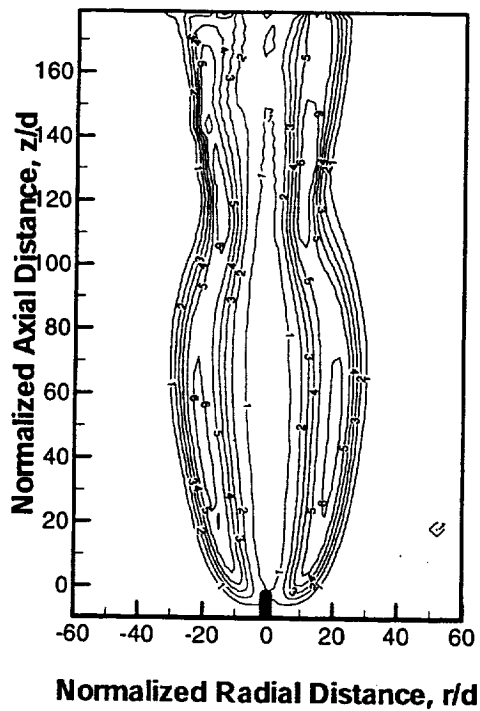


Fig. 3a Angular Deflection Contours in Earth-g, $Re=1300$

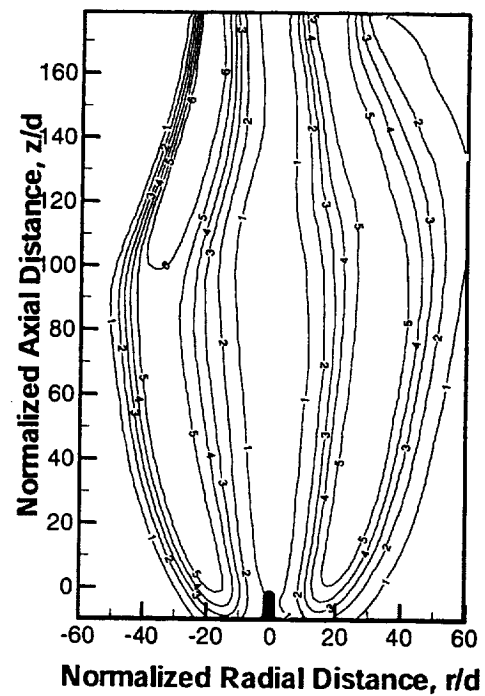


Fig. 3b Angular Deflection Contours in Micro-g, $Re=1300$

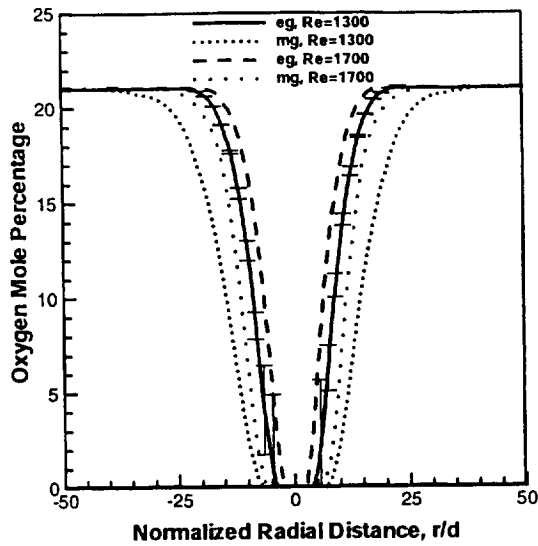


Figure 4. Profiles of Oxygen Concentration, $z/d=20Re$

As discussed above, a downstream shift of the transition region in microgravity might be caused by the increased separation distance between fuel jet and flame sheet. The oxygen concentration profiles in Fig. 8 show that this might not be the case. In Fig. 8, the dilution is shown to narrow the profiles and to increase

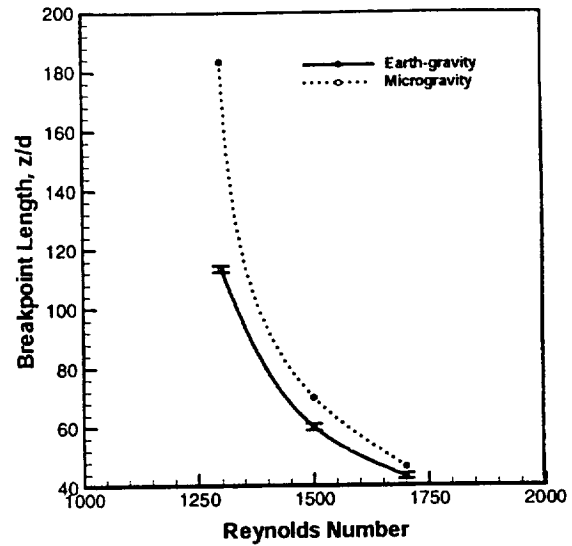


Figure 5. Breakpoint Length vs Reynolds Number

the radial gradients, both in earth and microgravity. Unlike with the pure fuel, the flame radius with diluted fuel is affected only marginally by the buoyancy. Thus, the result suggests that the buoyant flow acceleration is the primary cause for the early breakdown of fuel-jet shear layer in earth-gravity flames.

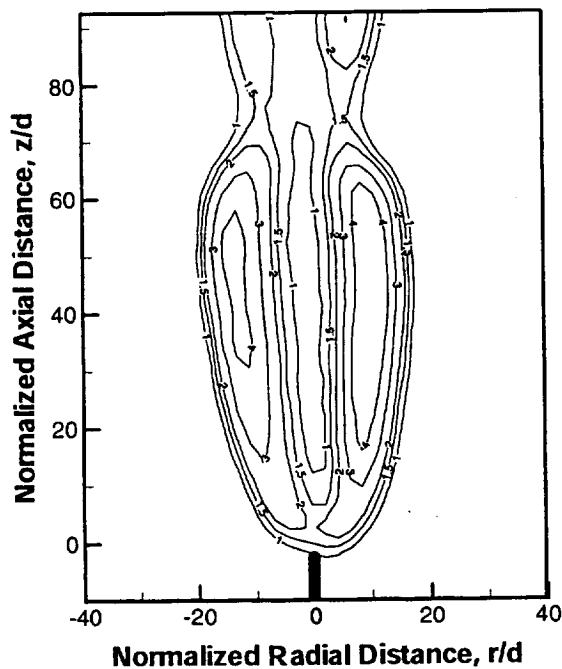


Fig. 6a Angular Deflection Contours in Earth-g, 40% He

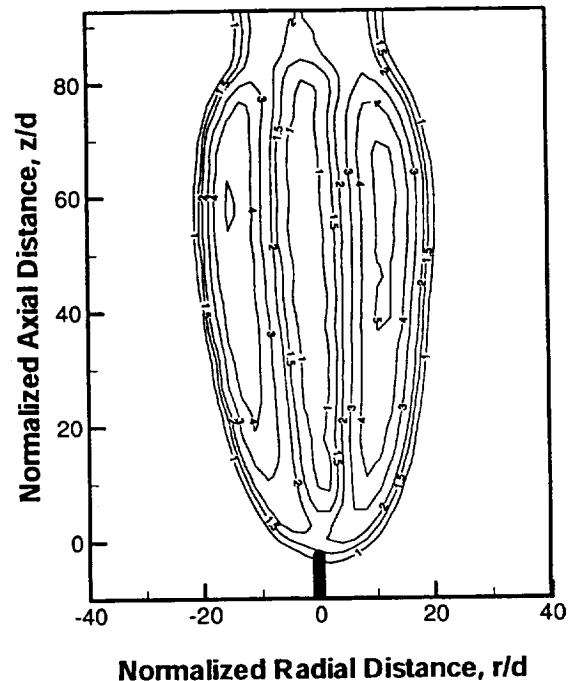


Fig. 6b Angular Deflection Contours in Micro-g, 40% He

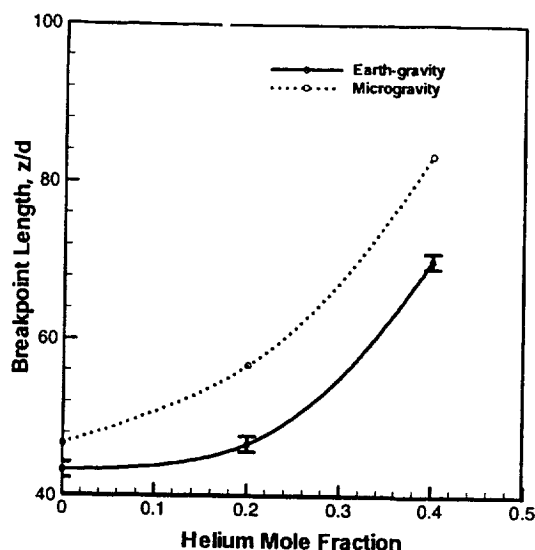


Figure 7. Breakpoint length vs Helium Mole Fraction

Conclusions

Experiments were conducted in the 2.2-s drop tower to evaluate buoyancy effects on transition from laminar to turbulent combustion in momentum-dominated hydrogen jet diffusion-flames. The fuel was discharged at jet exit Reynolds numbers below the critical Reynolds number for turbulent pipe-flow. Both earth and microgravity flames transitioned, evidently by the instability in the shear layer of the fuel jet. The Reynolds number effect on breakpoint length in microgravity was similar to that observed in earth gravity. The breakpoint length increased in the absence of gravity, suggesting laminarization of the fuel jet in microgravity. Results suggest that a transitional flame at low Reynolds numbers in earth gravity might remain laminar in microgravity. Buoyancy effects were also present in hydrogen flames diluted with helium.

Acknowledgements

This work was supported by the NASA Microgravity Science and Application Division, grant NAG3-1594.

References

1. Hottel, H.C., and Hawthorne, W.R., *Third Symposium (International) on Combustion*, The Combustion Institute, 1953, pp.254-266.
2. Takeno, T., and Kotani, Y., *Progress in Astronautics and Aeronautics*, AIAA Inc., New York, 1978, vol. 58, pp.19-35.

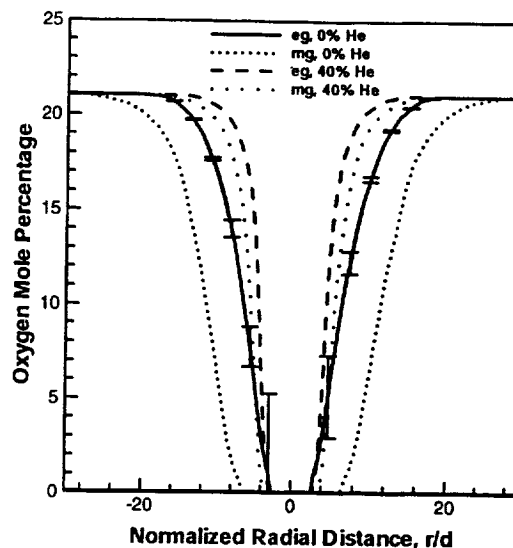


Figure 8. Profiles of Oxygen Concentration, $Re=1700$

3. Gaydon, A.G., and Wolfhard, H.G., *Flames, Their Structure, Radiation and Temperature*, Chapman and Hall, London, 1970, pp. 137-139.
4. Takahashi, F., Mizomoto, M., and Ikai, S., *Combustion and Flame*, 48:85-95 (1982).
5. Coats, C.M. and Zhou, H., *Twenty-Second Symposium (International) on Combustion*, The Combustion Institute, 1988, pp.685-692.
6. Yule, A.J., Chigier, N.A., Ralph, S., Boulderstone, R., and Ventura, J., *AIAA Journal*, 19:752-760 (1981).
7. Chen, L.-D., Vilimpoc, V., Goss, L.P., Davis, R.W., Moore, E.F., and Roquemore, W.M., *Twenty-Fourth Symposium (International) on Combustion*, The Combustion Institute, 1992, pp. 303-310.
8. Takeno, T., *Twenty-Fifth Symposium (International) on Combustion*, The Combustion Institute, 1994, pp. 1061-1073.
9. Hedge, U., Zhou, L., and Bahadori, M.Y., *Combustion Science and Technology*, 1994, 102:95-113.
10. Greenberg, P.S., Klimek, R.B., Buchele, D.R., *Applied Optics*, 34:3810-3822 (1995).
11. Al-Ammar, K.N., *Scalar Measurements and Analysis of Hydrogen Gas-Jet Diffusion Flames in Normal Gravity and Microgravity*, Ph.D. Dissertation, University of Oklahoma, 1998.